

Effect of Aggressive Media on the Corrosion Behavior Dissimilar Welding of 308L Stainless Steels Deposited on Carbon Steel

Amany Nagy Kamel¹, Eltohamy. R. Elsharkawy¹, A. F. Waheed²

¹Quality control and quality assurance department Egyptian nuclear and radiological regulator authority (ENRRA)

² Metallurgy Department , Nuclear Research Center, Atomic Energy Authority, Cairo, Egypt

Corresponding Author: Amany Nagy Kamel

ABSTRACT :The weld should have a corrosion / oxidation resistance equal to the least resistant base metal being joined. It is fortunate that in most all instances the weld will be of a higher alloy content (better corrosion and oxidation resistance) than the least resistant base metal being joined.

In this research paper , the microstructure and corrosion behavior in an aggressive media namely NaCl 3% of austenite stainless steels 308L (308L SS). Weld metal on carbon steel in the as weld condition and some specimens were aged at 550° C for different times, 50, 500 and 1000hr were studied. It was shown that corrosion measurements can be used for a proper evaluation of the quality of weld material and for the prediction of whether or not the suitable material. In this study, electrochemical techniques anodic polarization and metallographic analysis were used to study the corrosion of a weld material of austenitic stainless steels 308L. Based on surface and electrochemical analyses, it was shown that that corrosion occurrence was the result of the simultaneous activity of corrosion in ferrite and austenite material ,

KEYWORDS: Stainless steel (AISI 308L), carbon steel, corrosion, aging and ferrite numbers

Date of Submission: 30-05-2019

Date of acceptance: 14-06-2019

I. INTRODUCTION

The microstructures of austenitic stainless steels have been the object of considerable renewed interest within the last few years because the mechanical properties and corrosion behavior of this alloy are basically determined by the complicated as welded microstructures [1-3]. The complex structures result from not only the solidification behaviour but the subsequent solid state transformation which are controlled by composition and cooling rates. A welding process and procedure capable of producing welds of low dilution is beneficial. This is consistently obtainable with SMAW (stick welding) [4-7]

When a dissimilar metals welding (DMW) is in an environment where the liquid can be an electrolyte, the weld metal should be cathodic to more corrosion resistant than both base metals. If the weld is anodic (less corrosion resistant), it can suffer accelerated galvanic corrosion due to area effects [8]. Austenitic stainless steel welds exhibit some degree of susceptibility to localized corrosion, pitting and crevice corrosion, and in many cases, it is the limiting factor in stainless applications [9-12].

The connections dissimilar metals are prone to frequent failures. These problems are attributed to the difference in the mechanical properties across the weld, the coefficients of thermal expansion of the two types of steels and the resulting at the interface [13]. It must be considered the specific application as corrosion effects might have little significance in some applications while strength differences may be of far greater importance [14]. A welding process and procedure capable of producing welds of low dilution is beneficial. A common example would be welds between carbon steel and (308L SS) with an austenitic structure. Stainless steels are used extensively in the nuclear, battery, agricultural, automotive, and defense industries because of their excellent strength, oxidation characteristics and acceptable corrosion resistance [15, 16]

In this paper, the effect of the aggressive medium, 3% NaCl on the corrosion behavior of this layer of stainless steel 308L deposited on carbon steel was examined, by conducting metal corrosion tests, microscopic structure and measuring the hardness values of these layers deposited on carbon steel was also studied.

II. MATERIALS AND METHODS

2.1 The Materials and Surface Preparation

The type of electrodes E-308L of class AWS (American Welding Society) was used in the welding experiments, with diameter $\phi = 4$ mm. The chemical composition of the plates and electrode used are shown in Table(1).

Electrode type AWS E 308L welding process with SMAW with one pass. The welding current is 120~140A. Polarity DCEP and welding voltage is 60 V.

Table (1) the chemical composition of the plates and electrodes

Element	Carbon steel (CS)	E308L
C	0.2	<0.003
Si	0.23	0.8
Mn	1.37	0.8
Cr	0.01	19
Ni	0.01	10
Mo	0.005	-
P	0.02	-
S	0.008	-
Fe	Basis	Basis

2.2 Metallographic

The microstructure examination for the weld (308L) and carbon steel for as weld conditions and after aging were examined. The specimens were prepared by grinding under water on rotating disc, using abrasive paper with grades ranging from 180 to 2000. Then polished to mirrored surface by using diamond paste with grades 3 and 1 micron. Specimens were rinsed with alcohol and dried with hot air. The optical microscope (OM) was used for microstructural examination.

2.3 Microhardness

A Vickers microhardness testing machine with 300g and the indentation time was 30 second was used to measure at least seven microhardness values on the three region WM, HAZ and CS and then takes the mean value, as weld and after aging conditions.

2.4 Electrochemical Corrosion

The electrochemical corrosion behavior of as-weld, and after heat treatment for 50 hr, 500 hr and 1000 hr at 550 °C conditions, the samples was studied by applying the Potentiodynamic polarization technique using a potentiostat interfaced to a computer and a three-electrode cell with the working electrode of exposed area 100 mm², a saturated calomel reference electrode (SCE), carbon electrode as counter electrode. The testing media was 3% NaCl prepared from double distilled water and reagent grade salt. The surface area of 308L St.St is equal to (carbon steel) CS area which is immersion in the test solution; the rest of CS was covered with plastic tap.

III. RESULTS AND DISCUSSION

3.1 Microstructure and Solidification of Material

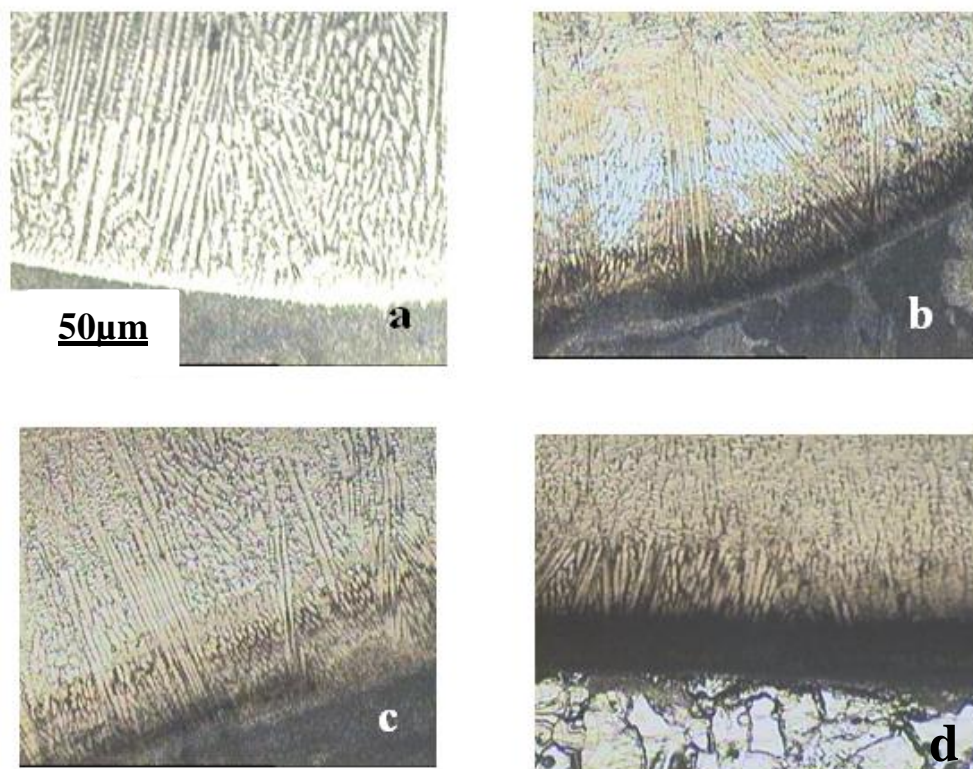
The base metal microstructure differed from the microstructure of the weld metal Figure(1). For commercial 300-series stainless steels the weld metal solidification mode can be determined from the Cr_{eq}/Ni_{eq} ratio. For 308L austenite stainless steel a (Table 1) $Cr_{eq}/Ni_{eq} = 1.92$, according to Schaeffler diagram [17,18], solidification mode FA ($1.48 \leq Cr_{eq}/Ni_{eq} \leq 1.95$). The solidification behaviour of stainless steel weld metal can be classified into four solidification modes (A, AF, FA, and F) according to its general microstructure and delta ferrite morphology. In the case of A mode, the weld metal completely solidifies to austenite. In AF mode, austenite is the leading phase and delta ferrite, if any, solidifies intergranularly from the rest melt. On the other

hand, in FA mode welds delta ferrite is the leading phase and austenite solidifies from the rest melt. At lower temperature the majority of ferrite is transformed to austenite by an equiaxial or acicular mechanism, depending on the supercooling of delta ferrite. In F mode, the weld metal solidifies completely to delta ferrite, and austenite is precipitated from the solid ferrite at lower temperatures[19-21]

The delta ferrite content in the weld metal plays an important role in determining the fabrication and service performance of the welded structures. The ferrite morphology will depend on the weld section viewed. David[22]observed four distinct types of ferrite morphology in AISI 308 stainless steel with a delta ferrite content from 9 to 15 %: vermicular, lacy, acicular and globular. Variations in ferrite morphology are related to the weld metal composition, ferrite content, and ferrite distribution as a result of thermal cycling during subsequent weld passes.

The microstructure of stainless steels 308L weld metal deposited on carbon steel in the as weld condition and aged specimens at times 50,500 and 1000 hr at 550°C are shown in Figure(1)

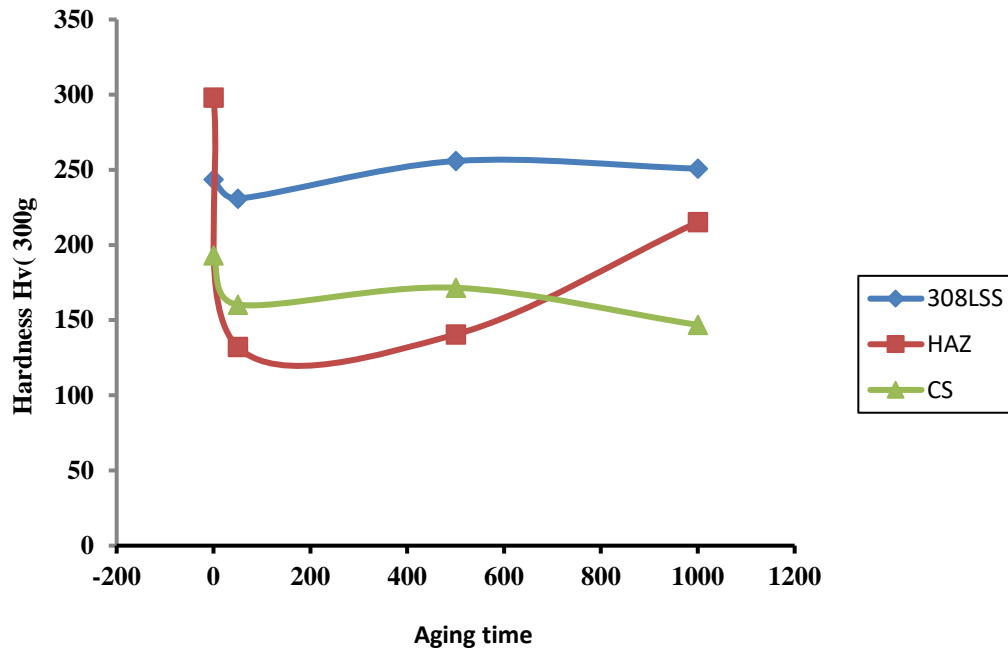
For stainless steel, chromium and molybdenum carbides precipitate along the grain boundaries during aging. As the carbides grow, carbon diffuses faster than chromium from the matrix to the grain boundaries. In doing so, chromium in the vicinity of the grain boundaries is drawn to form carbides. The phenomenon is commonly referred to as sensitization of stainless steel. Since chromium is one of the major elements providing resistance to corrosion, the depleted regions will be susceptible to corrosion attack.



Figure(1)The microstructure features of (308LSS) weld metal deposited on carbon steel (a) as weld (b) 50 hr (c) 500 hr and (d) 1000 hr ,aging at 550°C

3.2 Microhardness

The mean values of seven microhardness measurements on the three regions WM (308LSS), HAZ and CS were taken before and after aging at 550°C as shown in Figure(2). The microhardness values after aging were negligibly lower than microhardness values for as-welded WM and CS, the microhardness values of the weld metal were higher than CS. The remarkably higher hardness values for the weld metal could be accounted for its chromium content of about 19.0 wt.% which was higher than in the CS. This is in agreement with the results of Ohkubo et al. [23] investigated the effect of alloying elements on the mechanical properties of austenitic stainless steel. Increased weld metal hardness could also be due to the heat input from welding, melting and solidification of the area.



Figure(2)The effect of aging time on microhardness measurement on the three region WM(308LSS),HAZ and CS.

3.3 Ferrite Number

The Schaeffler diagram[24] Figure (3),DeLong diagram[25] and the WRC-1992 diagram[26] can be used to predict weld metal and transition region microstructure during dissimilar metal welding of stainless steels. Table (2)show the FN of weldment 308L by using the three diagrams.

The delta ferrite contentdecreased with the increasing aging temperature[19].

Table(2)show the FN of weldment 308L by using the three diagrams

Constitution Diagram	Cr _{eq} and Ni _{eq}	Cr, Ni Equivalent 308L	FN 308L
Shaefflerdiagram[24] Figure (3)	Cr _{eq} =Cr+Mo+1.5 Si Ni _{eq} = Ni+30C+0.5Mn	Cr eq. =20.2 Ni eq=10.49	20
DeLong diagram [25]	Cr _{eq} =Cr+Mo+1.5 Si Ni _{eq} = Ni+30C+30N+0.5Mn	Cr eq=20.2 Ni eq=10.49	16
WRC 1992 [26]	Cr _{eq} =Cr+Mo Ni _{eq} =Ni+35C+20N+ 0.25 Cu	Cr eq=20.2 Ni eq=10.105	18

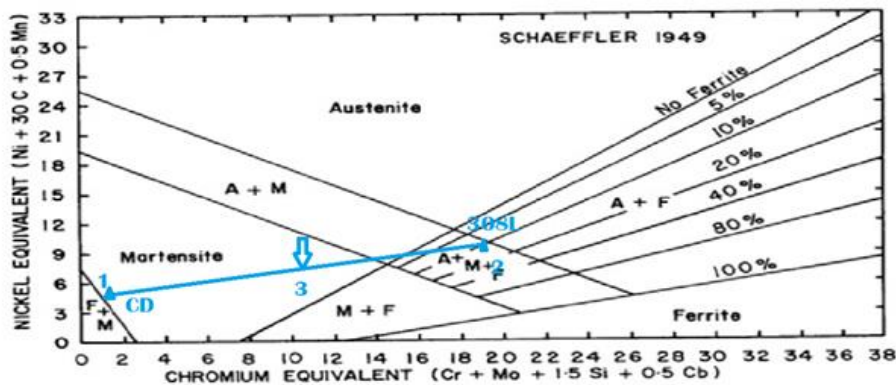


Figure (3) Schaeffler diagram [24]

By using Schaeffler diagram, we can be followed in predicting the first-pass weld microstructure for use 308L SS filler metals are used.

Figure (3) shows that the tie-line between the filler metal composition (308LSS) point 1 and the base metal point 2 that ferrite will be present 20%, unless dilution 50% point 3 by the base metals is extremely high, in which case, fuel martensite, not ferrite. Tie-line can also be used to predict the microstructure in the transition region at the fusion boundary. All these microstructures can be expected in a narrow region between the base metal HAZ and the fully mixed weld metal.

3.4 Corrosion Behavior of the Welded Material

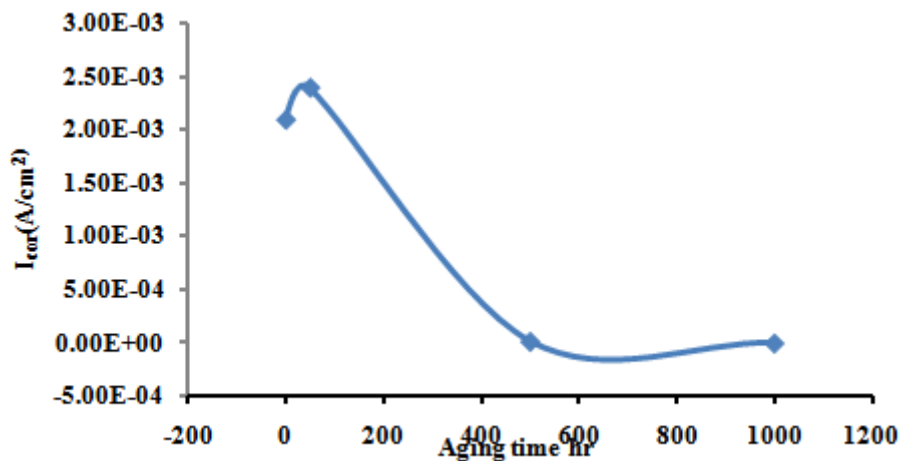
The corrosion current density I_{corr} and corrosion potential E_{corr} austenite stainless steels 308L, which were determined by potentiodynamic technique are shown in Table (3).

From these data, one may generally evaluate the corrosion behavior of austenite stainless steels 308L at different aging conditions.

Table (3) Corrosion potential E_{corr} and corrosion current density I_{corr} for austenite stainless steels 308L

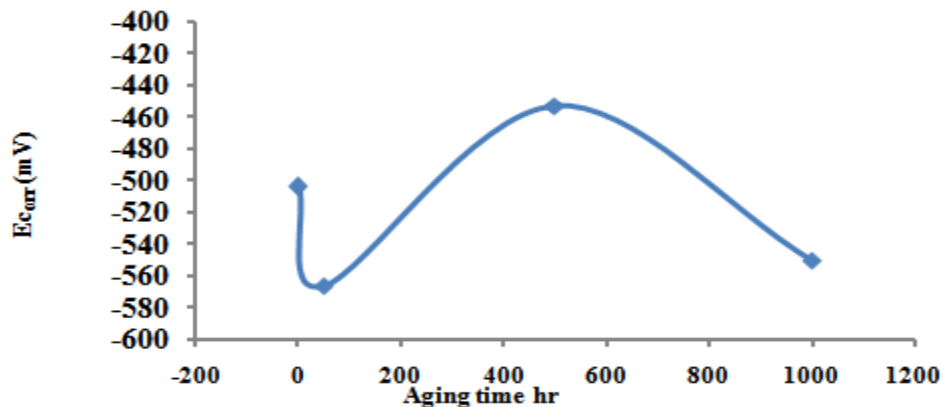
Aging condition	E_{corr} (mV)	I_{corr} (A/cm ²)
As weld	-504	2.1E-3
50hr	-566	2.4E-3
500hr	-453	17.21E-6
1000hr	-550	1.42E-6

The variation of corrosion current with increasing aging times shown in Figure (4). From the curve it is clear that the corrosion current increased on aging time 50hr and then decreased. The maximum corrosion current was recorded for aging at 50hr. This implies that the welding austenitic material was affected by aging time [27-28].



Figure(4) Effect of aging time on corrosion rate of 308L SS aged at 550 C

Effect of aging time on corrosion potential of 308L stainless steel specimens aged at 550C is illustrated in Figure(5),an increase in potential in the more reactive direction occurred after 50 hr of aging, but the rate of increase was much faster at 475mV. The most negative values of potential were found to occur upon aging for 50 hr. The maximum value at 500 hr, the potential then gradually decreased.



Figure(5) Effect of aging time on corrosion potential of 308L SS aged at 550° C.

Potentiodynamic polarization curves for specimens (308LSS. and CS) for as weld condition and specimens aged at times 500 and 1000 hr at 550 °C in 3% NaCl solution with neutral pH are shown in Figures (6-8).

In Figure (6) for as weld specimen the corrosion current density I_{corr} is 2.1E-3 A/cm², the current density increases moderately till -400 mV, after that the current density increases abruptly till the end of the run, which may be due to pits formation .

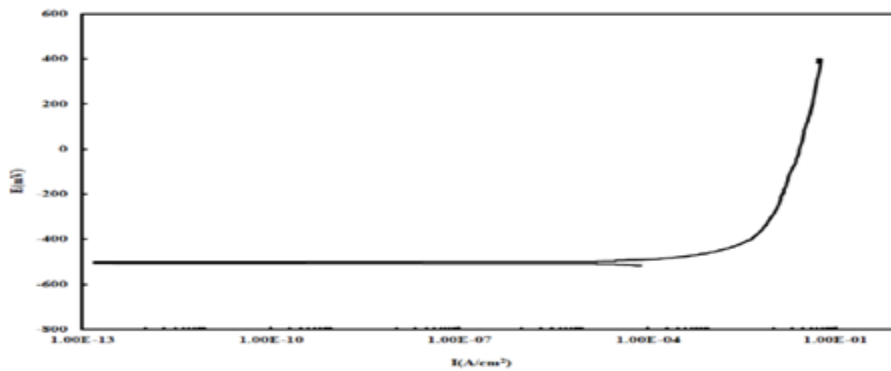


Figure (6) Potentiodynamic polarization curves of specimen (308L SS and CS) for as weld condition

Potentiodynamic polarization curves shows that the current density increases with increasing the applied potential till reaches almost constant value. This can be interpreted to the changes on the surface of the alloy.

Figure (7) shows the anodic polarization curve for specimen (308L SS and CS) aged for 500 hr at 550 °C, the corrosion current density I_{CORR} is $17.21E-6A/cm^2$, the current density increases moderately till -350 mV in this case the current density increases steadily with content rate to the end of the experiment.

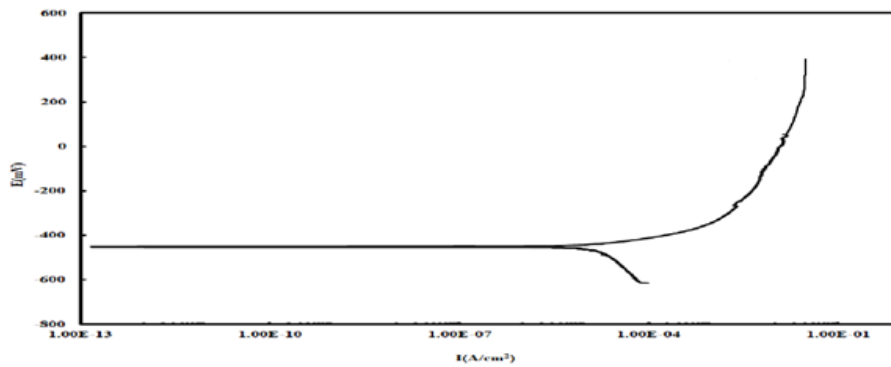


Figure (7) Anodic polarization curve in 3%NaCl solution of sample (308L SS and CS) aging for 500 hr at 550°C

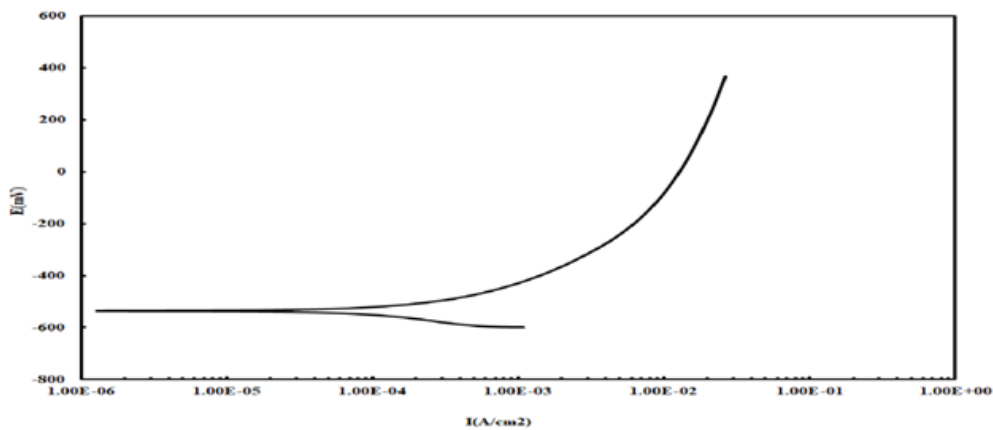


Figure (8) Anodic polarization curve in 3%NaCl solution of sample (308L SS and CS) aging for 1000 hr at 550°C

Figure (8) shows the anodic polarization curve for specimen (308L SS and CS) aged for 1000 hr. at 550°C, the corrosion current density I_{CORR} is $1.42E-3A/cm^2$, the current density increases moderately till -400 mV in this case the current density rapidly increases after corrosion potential.

The above results show that the corrosion performance of 308L stainless steel is highly dependent on aging temperature 550°C and time through the formation of reversed austenite, ferrite and molybdenum and chromium carbides.

The loss in corrosion resistance in stainless steel has been explained by the well known 'chromium depletion theory'. For 308L stainless steel, chromium and molybdenum carbides precipitate along the grain boundaries during aging. As the carbides grow, carbon diffuses faster than chromium from the matrix to the grain boundaries. In doing so, chromium in the vicinity of the grain boundaries is drawn to form carbides, resulting in chromium depleted zones. The phenomenon is commonly referred to as sensitisation of stainless steel. Since chromium is one of the major elements providing resistance to corrosion, the depleted regions will be susceptible to corrosion attack. However, if the aging time is prolonged, the sensitisation effect will eventually disappear as a result of chromium diffusion back from the matrix into the depleted zone, a phenomenon known as healing. The speed of sensitisation in stainless steels containing martensite is generally much more rapid, because the carbides form quickly within the martensitic laths and along the lath boundaries. Aging of the chromium depleted zone in these steels also occurs more rapidly and is attributed to the faster chromium diffusion in bcc martensite than in fcc austenite [29]. This can therefore explain the corrosion behavior of specimens aged at 550°C, so the change in corrosion rate at 550 °C with the changing of time can be due to high volume fraction of reversed austenite [30] and decreased delta ferrite content with the increasing annealing temperature. [19]

IV. CONCLUSIONS

The influence of morphology and corrosion behavior in 3% NaCl concentration, SS 308L thin films deposited on carbon steel were studied, the following conclusions can be adopted:

1. Schaeffler diagram the weld microstructure for use 308L SS fillers metals can be expected use 308L SS fillers metals can be expected. Close to the fusion boundary, the SS clad region consisted of a narrow zone of fine dendrites of ferrite and austenite.
2. Anodic polarization curves of specimens (308L SS and CS) for as weld condition and aging times 50, 500 and 1000 hr at 550 °C in 3% NaCl solution with neutral pH were studied. The major corrosion type that has been observed for all samples was localized corrosion.
3. The corrosion current density (I_{corr}) of the different conditions of the 308L SS varied in a very wide range from is $2.4 \times 10^{-3} \text{ A/cm}^2$ to $17.2 \times 10^{-6} \text{ A/cm}^2$ and the highest corrosion current density (I_{corr}) is for as weld condition. By Schaeffler diagram the weld microstructure for use 308L SS fillers metals can be expected. Close to the fusion boundary, the SS clad region consisted of a narrow zone of fine dendrites of ferrite and austenite.

REFERENCES

- [1]. Fu, J. W., Y. S. Yang, J. J. Guo, and W. H. Tong. "Effect of cooling rate on solidification microstructures in AISI 304 stainless steel." *Materials Science and Technology* 24, no. 8 (2008): 941-944.
- [2]. Brooks, J. A., and A. W. Thompson. "Microstructural development and solidification cracking susceptibility of austenitic stainless steel welds." *International Materials Reviews* 36, no. 1 (1991): 16-44.
- [3]. Siegel, Ulrich, Heinz-Joachim Spies, and Hans-Joachim Eckstein. "Effect of solidification conditions on the solidification sequence of austenitic chromium-nickel stainless steels." *Steel Research* 57, no. 1 (1986): 25-32.
- [4]. Hunter, A., and M. Ferry. "Phase formation during solidification of AISI 304 austenitic stainless steel." *Scripta Materialia* 46, no. 4 (2002): 253-258.
- [5]. Ferrandini, P. L., C. T. Rios, A. T. Dutra, M. A. Jaime, P. R. Mei, and R. Caram. "Solute segregation and microstructure of directionally solidified austenitic stainless steel." *Materials Science and Engineering: A* 435 (2006): 139-144.
- [6]. Wright, Richard N., John E. Flinn, Gary E. Korth, Jung Chan Bae, and Thomas F. Kelly. "The microstructure and phase relationships in rapidly solidified type 304 stainless steel powders." *Metallurgical Transactions A* 19, no. 10 (1988): 2399-2405.
- [7]. Brooks, J. A., J. C. Williams, and A. W. Thompson. "Microstructural origin of the skeletal ferrite morphology of austenitic stainless steel welds." *Metallurgical Transactions A* 14, no. 7 (1983): 1271-1281.
- [8]. Rajaković-Ognjanović, V., and Branimir N. Grgur. "Corrosion of an austenite and ferrite stainless steel weld." *Journal of the Serbian Chemical Society* 76 (2011): 1027-1035.
- [9]. Cui, Y., and Carl D. Lundin. "Austenite-preferential corrosion attack in 316 austenitic stainless steel weld metals." *Materials & design* 28, no. 1 (2007): 324-328.
- [10]. Rajaković-Ognjanović, V., and Branimir N. Grgur. "Corrosion of an austenite and ferrite stainless steel weld." *Journal of the Serbian Chemical Society* 76 (2011): 1027-1035.
- [11]. Joseph, A., Sanjai K. Rai, T. Jayakumar, and N. Murugan. "Evaluation of residual stresses in dissimilar weld joints." *International Journal of Pressure Vessels and Piping* 82, no. 9 (2005): 700-705.
- [12]. Gooch, T. G. "Corrosion behavior of welded stainless steel." *Welding Journal-Including Welding Research Supplement* 75, no. 5 (1996): 135s.
- [13]. Lu, B-T., Z-K. Chen, J-L. Luo, B. M. Patchett, and Z-H. Xu. "Stress corrosion crack initiation and propagation in longitudinally welded 304 austenitic stainless steel." *Corrosion engineering, science and technology* 38, no. 1 (2003): 69-75.
- [14]. Fang, Z., Y. Wu, R. Zhu, B. Cao, and F. Xiao. "Stress corrosion cracking of austenitic type 304 stainless steel in solutions of hydrochloric acid+ sodium chloride at ambient temperature." *Corrosion* 50, no. 11 (1994): 873-878.

- [15]. Rodriguez-Marek, D., D. F. Bahr, and M. Pang. "Mechanical measurements of passive film fracture on an austenitic stainless steel." *Metallurgical and Materials Transactions A* 34, no. 6 (2003): 1291-1296.
- [16]. Lu, B. T., Z. K. Chen, J. L. Luo, B. M. Patchett, and Z. H. Xu. "Pitting and stress corrosion cracking behavior in welded austenitic stainless steel." *Electrochimica acta* 50, no. 6 (2005): 1391-1403.
- [17]. Suutala, N. "Effect of solidification conditions on the solidification mode in austenitic stainless steels." *Metallurgical Transactions A* 14, no. 1 (1983): 191-197.
- [18]. 18-Mohammed, Ghusoon, Mahadzir Ishak, SyarifahAqida, and Hassan Abdulhadi. "Effects of heat input on microstructure, corrosion and mechanical characteristics of welded austenitic and duplex stainless steels: A review." *Metals* 7, no. 2 (2017): 39.
- [19]. S. Kožuh1, M. Goji'c, L. Kosec"Mechanical properties and microstructure of austenitic stainless steel after welding and post-weld heat treatment" *Kovove Mater.* 47 (2009)253–262
- [20]. Woo, Insu, and Yasushi Kikuchi. "Weldability of high nitrogen stainless steel." *ISIJ international* 42, no. 12 (2002): 1334-1343.
- [21]. Boothby, R. M. "Solidification and transformation behaviour of niobium-Stabilized austenitic stainless steel weld metal." *Materials science and technology* 2, no. 1 (1986): 78-87.
- [22]. David, S. A. Ferrite morphology and variations in ferrite content in austenitic stainless steel welds. Oak Ridge National Lab., TN,(1981). p. 63.
- [23]. Ohkubo, Naoto, KatsuhisaMiyakusu, Yoshihiro Uematsu, and Hiroshi Kimura. "Effect of alloying elements on the mechanical properties of the stable austenitic stainless steel." *ISIJ international* 34, no. 9 (1994): 764-772.
- [24]. Schaeffler, A. L" Constitution diagram for stainless steel weld metal". *Meta Progress*(1949). 56(11): 680–680B.
- [25]. 25-Long, C. J., and DeLong, W. T."The ferrite content of austenitic stainless steel weld metal". *Welding Journal* (1973)52(7): 281-s to 297-s.
- [26]. Kotecki, D. J., and T. A. Siewert. "WRC-1992 constitution diagram for stainless steel weld metals: a modification of the WRC-1988 diagram." *Welding Journal* 71, no. 5 (1992): 171-178.
- [27]. Hasçalik, A., E. Ünal, and N. Özdemir. "Fatigue behaviour of AISI 304 steel to AISI 4340 steel welded by friction welding." *Journal of materials science* 41, no. 11 (2006): 3233-3239.
- [28]. Wang, Jun, Cong Li, Haohuai Liu, Hongshan Yang, Baoluo Shen, Shenji Gao, and Sijiu Huang. "The precipitation and transformation of secondary carbides in a high chromium cast iron." *Materials Characterization* 56, no. 1 (2006): 73-78.
- [29]. Robino, C. V., M. J. Cieslak, P. W. Hochanadel, and G. R. Edwards. "Heat treatment of investment cast PH 13-8 Mo stainless steel: Part II. Isothermal aging kinetics." *Metallurgical and Materials Transactions A* 25, no. 4 (1994): 697-704.
- [30]. Abdel-Karim, R., MM AL Dawood, IS EL Mahallawi, and MR EL Koussy. "Effect of thermal aging on pitting corrosion resistance of 16Cr–5Ni–1Mo precipitation hardening stainless steel." *Materials science and technology* 20, no. 12 (2004): 1573-1577.

Amany Nagy Kamel" Effect of Aggressive Media on the Corrosion Behavior Dissimilar Welding of 308L Stainless Steels Deposited on Carbon Steel" *American Journal of Engineering Research (AJER)*, vol.8, no.06, 2019, pp.184-191